https://doi.org/10.5194/egusphere-2022-565
Preprint. Discussion started: 19 August 2022

Development of an automated pump efficiency measuring system for ozonesonde utilizing the airbag type flowmeter

Tatsumi Nakano[1, a], Takashi Morofuji[2]

[1]Aerological Observatory, Japan Meteorological Agency, 1-2, Nagamine, Tsukuba-shi, Ibaraki 305-0052, Japan
[2]Atmosphere and Ocean Department, Japan Meteorological Agency, 3-6-9, Toranomon, Minato-city, Tokyo 105-8431, Japan
[a]Currently at: Fukuoka Regional Headquarters, Japan Meteorological Agency, 1-2-36, Ohori, Chuo-ku, Fukuoka-shi, Fukuoka 810-0052, Japan

Correspondence to: Takashi Morofuji (morofujitakashi@met.kishou.go.jp)

Abstract. We have developed a system to automatically measure the flow rate characteristics of the pump built in the ozonesonde, so called "pump efficiency", under various pressure situations emulating upper air conditions. The system consists of a flow measurement unit that uses a polyethylene airbag, a pressure control unit that reproduces a low-pressure environment, and a control unit that integrates and controls these, and enables fully automatic measurement. The Japan Meteorological Agency (JMA) has been operationally measuring the pump efficiency of the Electrochemical Concentration Cell (ECC) ozonesondes using the system since 2009, and has accumulated a lot of measurement data. From the multiple measurements of the same ozonesonde pump for around twelve years, we confirmed the long-term stability of the system's performance. The long-term measurement data also showed that the pump flow characteristics of ozonesondes differed among production lots. We evaluated the impacts of the variance in these characteristics on the observed ozone concentration data comparing with the reference ozone profiles, and found that the influences on total ozone estimation was about 4% to the maximum, the standard deviation per lot was about 1%, and the standard deviation among lots was about 0.6%.

1 Introduction

Ozone in the atmosphere protects the biosphere by absorbing harmful ultraviolet radiation. In order to monitor the destruction of the ozone layer due to the release of chemical substances caused by human activities, the World Meteorological Organization (WMO) has taken the lead in observing ozone profiles on a global scale (Smit et al., 2021).

Ozonesonde observations are the only means of directly obtaining the detailed vertical distribution of ozone from the troposphere to the lower stratosphere. The ozonesonde is a balloon borne measurement sensor to be flew up from the ground up to around 35 km high where the balloon bursts, while taking in the ambient air and measuring the amount of ozone by chemical method. The downlink of the data is taken care of by the radiosonde - also providing pressure, temperature, humidity and position measurements – the ozonesonde is coupled with.

Since around 2008-2010 (depending on the station), the Japanese Meteorological Agency (JMA) has been using the Electrochemical Concentration Cell (ECC)-ozonesonde developed by Komhyr (1969, 1971). The ECC-ozonesonde is also

https://doi.org/10.5194/egusphere-2022-565
Preprint. Discussion started: 19 August 2022

widely used in the world, about 80% of stations of WMO / the Global Atmosphere Watch (GAW) programs' ozone observing networks use this type (World Ozone and Ultraviolet Radiation Data Centre, "Dataset Information: OzoneSonde"). Historically, since 1968, JMA had observed the vertical ozone distribution with the KI solution and Carbon electrode type (KC)-ozonesonde developed at the Meteorological Research Institute of JMA.

An ozone sounding measurement originates from an ozone sensor unit (piston pump, motor, reaction cells, tubes, etc.) and is extended with the measurements taken from the coupled radiosonde unit (pressure sensor, temperature sensor, humidity sensor, GPS antenna, etc.) as shown in Fig 1. The ozone sensor unit uses a small piston pump to take the ambient air into the reaction cell and measures the electric current generated by the chemical reaction of the potassium iodide solution contained in the cell with the ozone in the sampling air. The ozone concentration is calculated from this electric current.

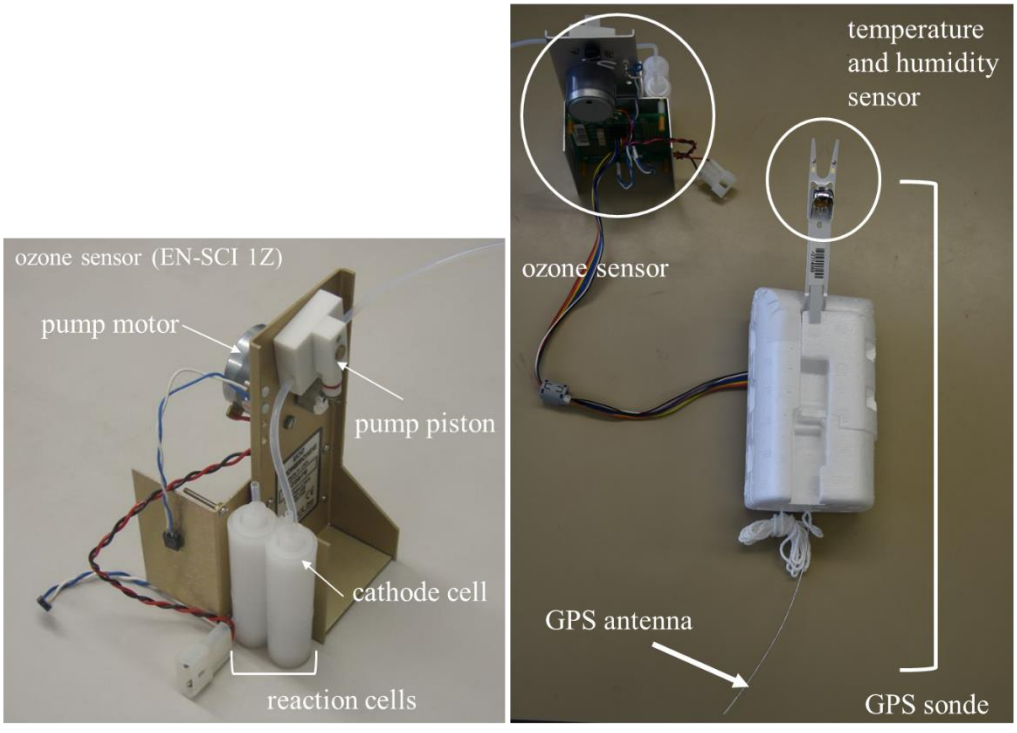

Figure 1: Appearance of the ozone sensor of the ECC type ozonesonde (left) and GPS sonde connected to the ozone sensor (right).

Figure 2 shows how the pump operates. Firstly, the ambient air taken into the pump is compressed until its pressure is balanced with the back pressure due to the hydraulic head pressure of the reaction cell and a Teflon rod in the reaction cell (1). The compressed air is then discharged to the cell by the force of the piston (2). When the piston is completely pushed in, there is a dead space inside the pump (3), and the compressed air remaining in it expands until it is balanced with the ambient air pressure (4). Then again, the force of the piston takes the ambient air into the pump (5). During the ozonesonde observation, this cycle is repeated. The back pressure could be assumed nearly identical at the ground level pressures and at lower pressures in the upper air, but the ambient air pressure is different along with the altitude. Under these conditions, the air taken in is more

https://doi.org/10.5194/egusphere-2022-565
Preprint. Discussion started: 19 August 2022

compressed in step (1) and the air in the dead space is more expanded in step (4). In other words, as the ambient air pressure decreases, the intake air volume (=pump flow rate) into the reaction cell reduces. As a consequence, the pump is affected by the ambient air pressure, which is called the pump efficiency.

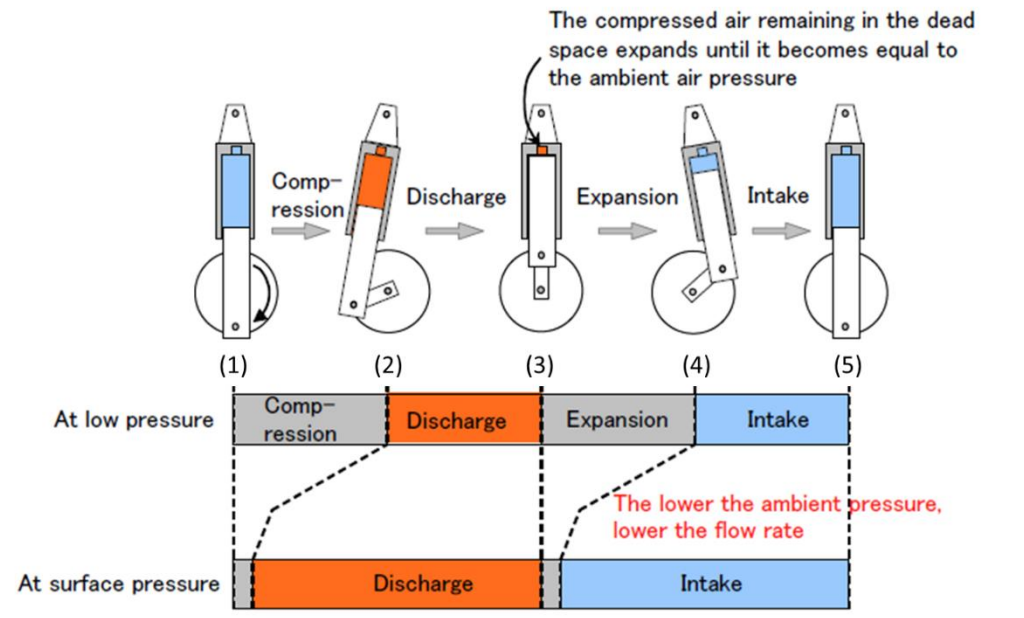

Figure 2: Explanation of how the piston pump operates during observation and how the dead space of the pump affects pump efficiency.

Based on laboratory pump flow measurements (Komhyr et al., 1986, 1995; Johnson et al., 2002), Smit and the panel for ASOPOS (2014) and Smit et al. (2021) provide useful tables of pump flow correction factors or pump flow efficiencies as a function of air pressure. These values are averaged from the experiments at the time of the ECC-ozonesonde development and the values recommended by the manufacturer. Causes of pump flow reduction (dead volume in the piston of the pump, pump leakage, hydraulic head pressure of the reaction solution in the reaction cell, etc.) might vary considerably between individual ozonesondes. In order to eliminate such observational uncertainty factors, it is necessary to accurately measure the pump efficiency of each ozonesonde in the preflight preparation.

Individual pump efficiencies have already been measured by research themes in the past. For example, the National Oceanic and Atmospheric Administration/Climate Monitoring and Diagnostics Laboratory (NOAA / CMDL) developed a silicone membrane flowmeter using silicone oil (Johnson et al., 2002), and showed that the conventionally used standard pump efficiency tables (Komhyr et al., 1986, 1995) were underestimated compared to the pump efficiencies of the currently manufactured the ECC-ozonesondes. Also, the University of Wyoming has measured individual pump efficiency using an airbag contraction type flowmeter equipped with an airbag and a gear pump with high pump efficiency (Johnson et al., 2002). However, as a pump efficiency measuring system is currently not commercially available, we developed such a system at the Aerological Observatory in Tateno, Japan. After examining various measurement methods, we adopted an airbag method for

https://doi.org/10.5194/egusphere-2022-565
Preprint. Discussion started: 19 August 2022

its easiness to control. The system was designed to perform the entire series of measurement automatically, in order to be able to obtain pump efficiency with uniform quality. Since 2009, we have installed this system at Tateno, Sapporo, Naha and Syowa stations in sequence. At these stations, the pump efficiency of 'each' individual ozonesonde has been measured operationally. Because of the operational ozonesonde measurement program in the last decade, we could build up a long time series of pump efficiency measurements at those sites.

In this paper, firstly in section 2, we introduce the outline of the automated pump efficiency measuring system. In section 3, the measurement method and procedures using this airbag type system are explained. The calculation of pump efficiency is described in section 4. Lastly in section 5, the statistical results of pump efficiencies obtained through the operational observation for this decade and the long-term stability estimates of the pump measurement system are shown.

2 Overview of the system

The automated pump efficiency measuring system is roughly divided into three parts: "Control unit", "Pressure control unit" and "Flow measurement unit". Figure 3 shows the conceptual diagram of the system, and Figure 4 shows its appearance. The control unit is designed to control the whole measurement system by PC with a module that communicates directly with peripheral equipment. The pressure control unit consists of a vacuum pump, a vacuum controller, and a digital barometer. The flow measurement unit consists of an air-bag type flowmeter in a vacuum desiccator that allows various pressure conditions down to 3 hPa.

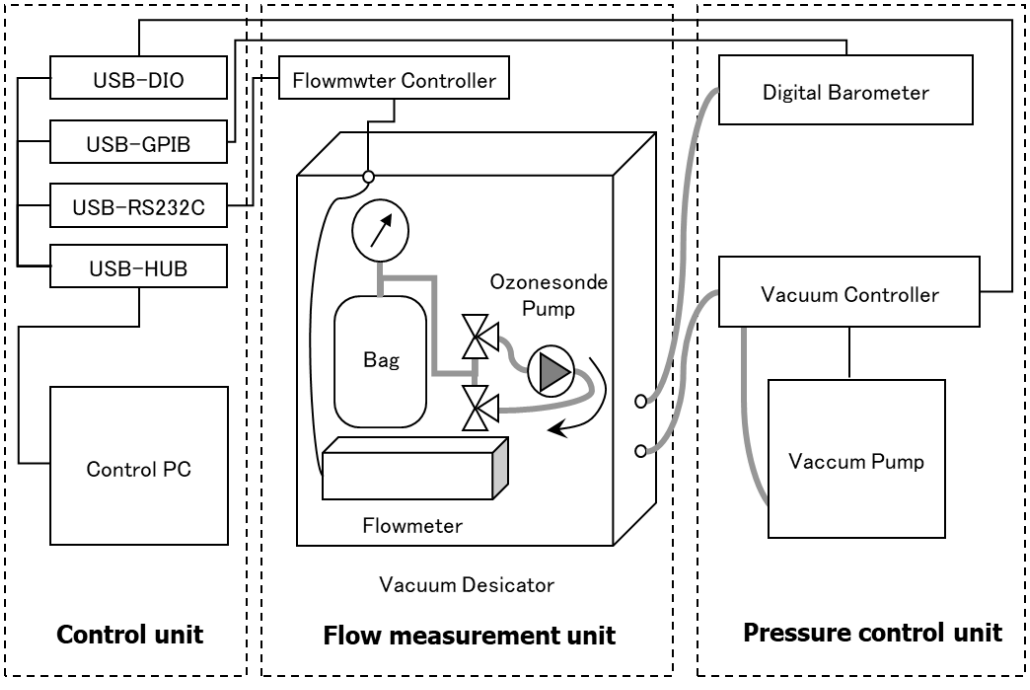

Figure 3: Schematics of the automated measurement system of the pump efficiency for the electrochemical concentration cell (ECC) ozonesonde.

https://doi.org/10.5194/egusphere-2022-565
Preprint. Discussion started: 19 August 2022

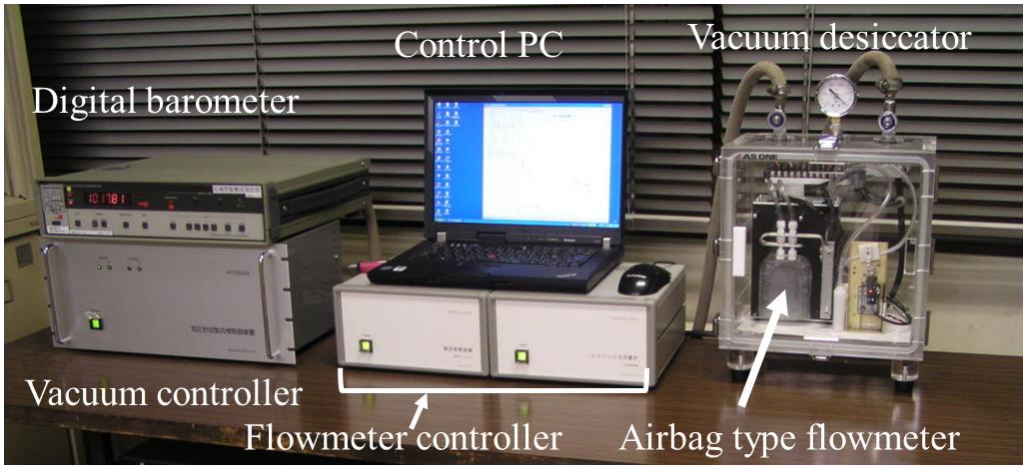

Figure 4: Picture of automated measurement system of the pump efficiency for the ECC ozonesonde.

The control unit consists of a Windows PC combined with various communication modules (DIO, GPIB, and RS232C) to control the entire system and collect measurement data. As these modules and the control PC are connected via USB, the system can be controlled by a general-purpose PC.

A program to control the system was developed as software running on Windows, and is used to control the pressure control unit and the flow measurement unit. The program also has the function to convert various measurement data acquired from the flow measurement unit at regular intervals into physical values and to collect the data together with other information such as the digital barometer.

The pressure control unit controls the air pressure in the vacuum desiccator to reproduce a low-pressure environment. During a balloon ascent, the ozonesonde is not only subjected to decreasing atmospheric pressure, but also to lower temperature conditions (as low as -60 to -80°C). For this reason, we initially tried to reproduce not only the low-pressure environment, but also the low-temperature environment. However, our pump efficiency measurements in a low-temperature environment showed that temperature does not have a linear relationship with pump efficiency, and even has a negligible effect, at least in the temperature range of real atmospheric conditions. For this reason, we decided to perform pump efficiency measurements by reproducing only the low-pressure environment. Since the exhaust limit of the unit is less than 3 hPa, the entire pressure range of ozonesonde measurements can be reproduced.

By manipulating the opening degree of the exhaust valve in the vacuum controller with the control program, the pumping speed of the vacuum pump, i.e., the decompression speed in the desiccator, can be adjusted. The pressurization speed can also be controlled by opening and closing the solenoid valve for atmospheric pressure release. With these adjustment functions, the air pressure in the desiccator can be maintained within approximately ± 0.1 hPa of the target air pressure by setting the decompression speed to zero during flow measurement performed at each specified air pressure. At the start of depressurization and pressurization, a series of procedures is required to avoid sudden air pressure changes in the desiccator, which might cause a backflow of oil from the vacuum pump to the desiccator. The control program has the function to execute them safely.

https://doi.org/10.5194/egusphere-2022-565
Preprint. Discussion started: 19 August 2022

The flow measurement unit consists of a vacuum desiccator, a flowmeter controller, and a control PC. Figure 5 shows the schematic diagram of the flow measurement unit.

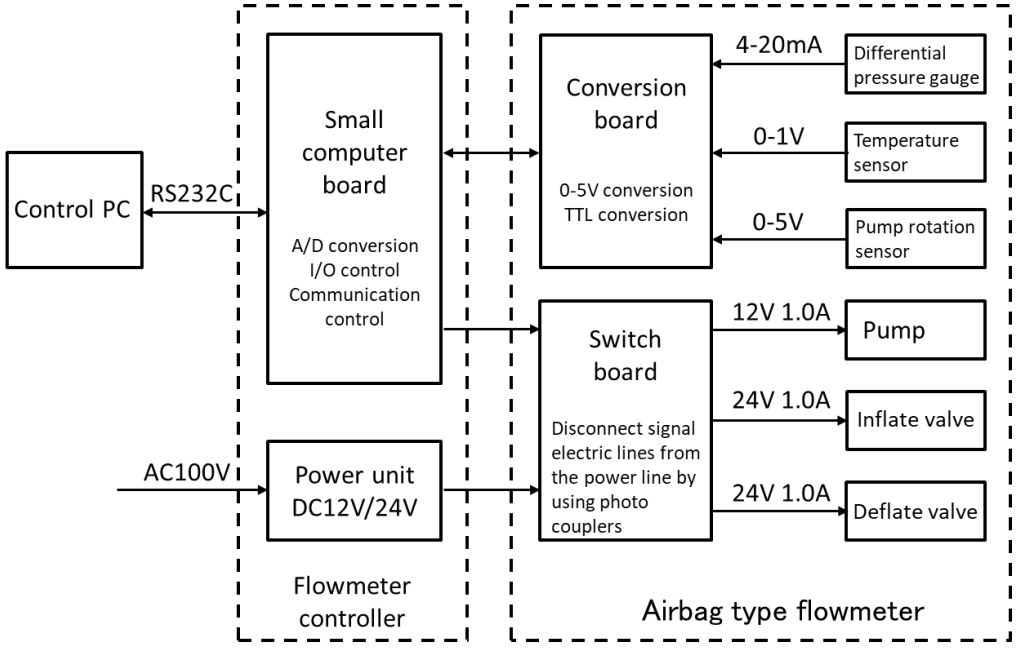

Figure 5: Schematic diagram of the flow measurement unit.

Inside the vacuum desiccator, the ozonesonde pump and an airbag type flowmeter are located. Flowmeter controller, which is set outside the vacuum desiccator, controls the flowmeter and acquires flow values of them.

The flowmeter controller supplies power to the flowmeter, monitors and controls the flowmeter status every millisecond using the built-in microcomputer (H8/3052F), and sends and receives control commands and measurement data between the control PC using RS232C. Due to the flowmeter controller taking care of time-dense control, the load of the control PC is largely reduced.

The airbag type flowmeter has a conversion board to adapt the output of various sensors to the input to a small computer board, and a switch board to control the power supply of the pump and solenoid valve. These power supply lines and signal lines are electrically isolated using photo couplers to reduce noise contamination of the signal lines. Figure 6 shows the piping connection diagram of the airbag type flowmeter. The inflate and deflate valves are fluororesin three-way solenoid valves, with NO (normally open) to COM (common) communication when not powered, and NC (normally closed) to COM communication when powered. By switching these valves alternately, the airbag air is taken in and out by the pump.

https://doi.org/10.5194/egusphere-2022-565
Preprint. Discussion started: 19 August 2022

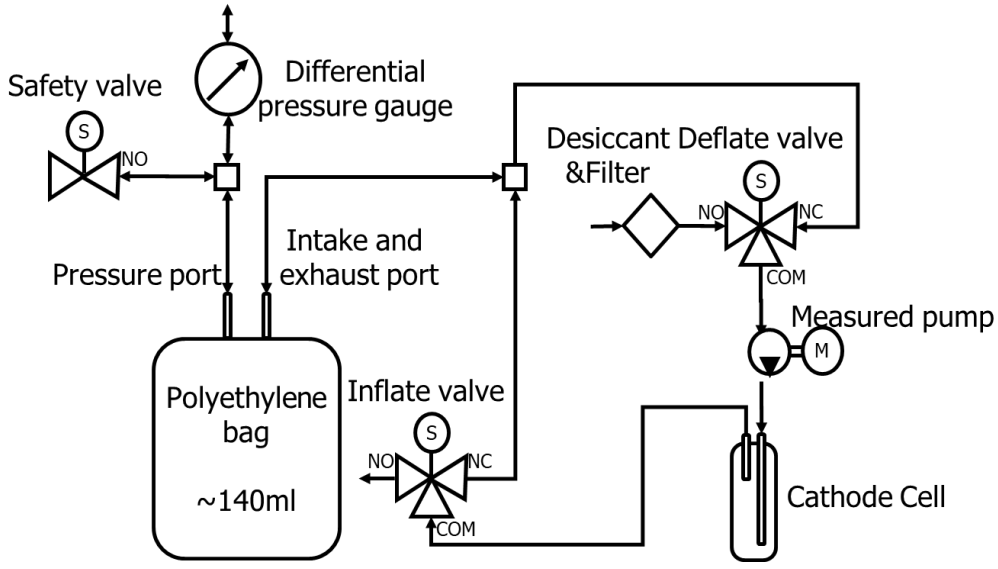

Figure 6: Piping connection diagram of airbag type flowmeter. The bag is made of polyethylene in a volume of 140 ml. The inflation and deflation of the bag is conducted by using two magnet valves. The pressure between the inside and outside of the bag is measured with a differential pressure gauge. Temperatures in the bag and pump are measured in thermometers. The revolving speed of the pump is measured in optical instrument.

The airbag is equipped with a port for differential pressure measurement separately from the intake and exhaust ports to ensure stable differential pressure measurement. A Setra Systems pressure transducer, Model 265, is used as the micro differential pressure gauge. It has a measurement range of ±1 hPa and an accuracy of ±1 %FS.

The material of the airbag must be able to deform with very weak force, be airtight, and have little elongation and shrinkage, and should be easy to work with or manipulate.. Among the available materials, polyethylene film with a thickness of 0.01 mm showed the best behaviour. In addition, wrinkles in the airbag as it repeatedly expands and contracts can cause erroneous measurements, so a smaller fluoroplastic film is placed inside the bag to prevent these. As a result of repeated prototyping, the airbag eventually took on a shape similar to that of an intravenous drip bag.

The main control and measurement items of the flow measurement unit are as follows.

- Pump ON / OFF control
- Control of flow path switching by inflate (deflate) valve
- Measurement of pressure difference between inside and outside of the airbag (differential pressure) （0.01hPa）
- Measurement of pump temperature, temperature in the desiccator, temperature in the airbag (thermistor placed in it) (0.1°C)
- Measurement of pump motor speed with a handmade digital tachometer attached to the ozone sensor (0.1 rpm) (The tachometer shines light on the rotating part of the pump and detects the reflected light to measure the number of revolutions. The rotating part is partially covered with a black sticker. When light hits the sticker, the light is not reflected, so the tachometer can measure a full revolution.)

https://doi.org/10.5194/egusphere-2022-565
Preprint. Discussion started: 19 August 2022

- Time interval measurement triggered by the specified differential pressure (1msec)

3 Method for measuring pump efficiency using the airbag method

3.1 Basic idea

The basic idea of estimating the pump flow rate (pumping power) using an airbag is to measure the inflation time from the most deflated state of the bag to the most inflated state, and the deflation time from the most inflated to the most deflated. Assuming the airbag internal volume V_{airbag} to be constant regardless of ambient pressure, the pump flow rate $S(p)$ at a given pressure p can be estimated with the averaged inflation and deflation time $t(p)$ as

$$S(p) = V_{airbag}/t(p). \quad (1)$$

The pump efficiency $k(p)$ at the given pressure p, which is defined as ratio of the pump flow rate to that estimated at the ground level pressure p_0, can be calculated as follows,

$$k(p) = S(p)/S(p_0) = (V_{airbag}/t(p))/(V_{airbag}/t(p_0)) = t(p_0)/t(p). \quad (2)$$

As this equation shows, we do not need to know the exact volume of the airbag.

On the other hand, we have to assess whether or not the airbag is fully inflated or deflated, in some way. Therefore, we use the differential pressure between the airbag's inside and outside. We set the threshold to +/- 0.8 hPa (+ during inflation and - during deflation); we will come back to this choice later in this paper. The flow will be switched by two valves shown in Fig. 6 when the differential pressure reaches the thresholds. Figure 7 shows the variation of the differential pressure with elapsed time, starting from the time of the maximum deflation. A series of measurements is made when the flow will be switched at the ground level pressure. Since the pump flow rate at the ground level is stable, we can consider the elapsed time to be equivalent to the internal volume of the airbag. During inflation and deflation, there seems to be a hysteresis effect (blue line) in which the relationship between the differential pressure and the content volume does not match, but when it is plotted folded around the time of maximum deflation (red line), it matches. This indicates that the inflation time and deflation time are equal, and the pump repeatedly takes in and exhaust a constant volume. We have performed multiple measurements on this and have confirmed that the folded and plotted differential pressure diagrams are always the same. From the above, thus, we conclude that the differential pressure during inflation and deflation each represent a certain airbag volume, and can determine the pump efficiency from equation (2) by measuring the time interval at which a certain differential pressure (hereinafter referred to as the differential pressure threshold) is detected.

https://doi.org/10.5194/egusphere-2022-565
Preprint. Discussion started: 19 August 2022

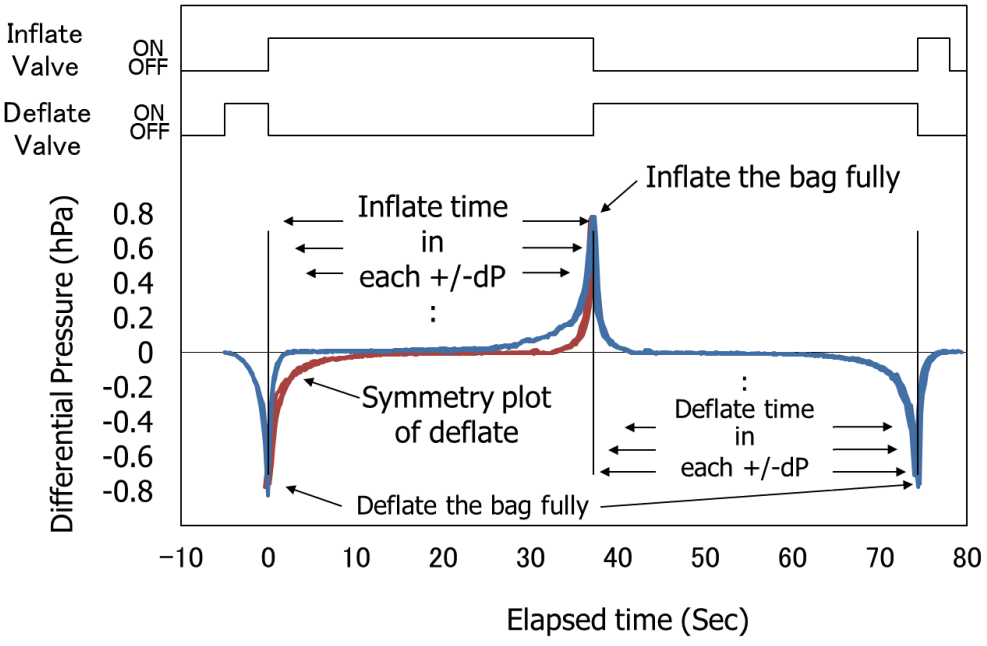

Figure 7: Schematics of pressure differences between the inside and outside of the bag as a function of lapsed time. A blue line represents plots of four-time average difference-pressure and the inflation/deflation of the bag is changed when the magnitude of difference pressure reaches 0.8 hPa. A red line is a symmetric reference line of deflation to the maximum inflation at an elapsed time of around 36 seconds. Also, on/off lines of inflation and deflation are plotted in the upper part of the panel.

Here, the pump correction factor, which is generally the reciprocal of the pump efficiency, is used in the ECC-ozonesonde observation. The factor obtained only from the time required for airbag inflation and deflation in the case of differential pressure Δp is expressed from equation (2) as follows,

$$pcf_0(p, \Delta p) = \frac{1}{k(p)} = \frac{t(p,\Delta p)}{t(p_0,\Delta p)}, \quad (3)$$

where $pcf_0(p, \Delta p)$ is the pump correction factor for differential pressure Δp at air pressure p and $t(p, \Delta p)$ is the time required to reach differential pressure Δp at air pressure p (p_0 is the ground level pressure). In practice, however, the effects of differences in differential pressure thresholds and temperature changes due to the heat generated by solenoid valves and pump motors can cause measurement errors, so we need to consider a correction method. The details are described in section 4.

3.2 Measurement sequence and measured value

In a series of measurements, the automated pump efficiency measuring system takes measurements at pressure levels: the ground level pressure, 500, 200, 100, 50, 30, 20, 10, 7, 5, 4, and 3 hPa. Measurements from inflation to deflation are performed 6 times at the ground level pressure and 4 times at other pressures. In each case, the first time is the "break-in" of the airbag at each atmospheric pressure, so the values after the second time are used as the measured values. The pump correction factor

https://doi.org/10.5194/egusphere-2022-565
Preprint. Discussion started: 19 August 2022

finally calculated is the average value of those values at the time of inflation and deflation. For each measurement, the system also acquires additional data as the time required for the differential pressure inside and outside the airbag to reach ±0.1, 0.2, 0.3, 0.4, 0.5, 0.6, 0.7, 0.8 hPa (+ during inflation, - during deflation), pump temperature, and temperature in the bag. After the cycle of measurements at the different pressure levels, six measurements at ground pressure are taken again to confirm reproducibility of the pump operation. The measurement pressure, the number of measurements, the differential pressure threshold, and other settings for this sequence of measurements can be changed in the control program.

3.3 Investigation of back pressure effect

The ECC-ozonesonde has a Teflon rod protruding from the bottom of the reaction cathode cell in order to guide the air intake tube from the pump properly into the reaction solution, by sliding the tubing over the Teflon rod. The Teflon rod could narrow the air flow and give pressure resistance. Additionally, in actual ozonesonde observations, the reaction cells are filled with solutions. Under these situations, the back pressure must affect the pump efficiency. Therefore, at the first step, we investigated the back pressure effect of the guiding Teflon rod and the reaction solution on the pump efficiency. In all measurement tests, we used the same ECC-type (EN-SCI 1Z) sensor. This section describes the results of the survey.

Figure 8 (a) shows the results of a comparison between the case where the pump is directly connected to the flowmeter from the exhaust port of the pump and the case where the air flow goes through an empty reaction cell. This experiment shows that the pump efficiency decreased (about -6% to the maximum at 3 hPa) by connecting through the cell, and the cell itself generated back pressure. This back pressure generation may be due to the thin line.

Next, we examined the relationship between the volume of the reaction solution and back pressure. However, if the pump efficiency is measured with the solution in the cells, the airbag type flowmeter will fail due to backflow caused by boiling of the solution during flow measurement especially under low pressure conditions. So, we used silicon oil with almost the same specific density as the reaction solution instead. Figure 8 (b) shows the results of a comparison between an empty reaction cell and an ECC-type standard reaction solution volume of 3 ml. From this result, we found that the load due to the reaction solution also reduced the pump efficiency (about -4% to the maximum at 3 hPa). We considered that the head pressure of the reaction solution causes this effect.

Figure 8 (c) shows the results of a comparison of pump efficiencies during inflation and deflation under the same load conditions. Normally, the intake speed and exhaust speed of the pump are the same, and the pump efficiency should be the same at the time of intake and exhaust, but the pump efficiency during deflation is always lower than that during inflation (about -8% to the maximum at 3hPa). Since the pump efficiency shows a change tendency depending on the ambient air pressure like the change due to other loads, we consider that an additional load, presumably the dead space of the pump (as explained in section 1), is responsible for it.

https://doi.org/10.5194/egusphere-2022-565
Preprint. Discussion started: 19 August 2022

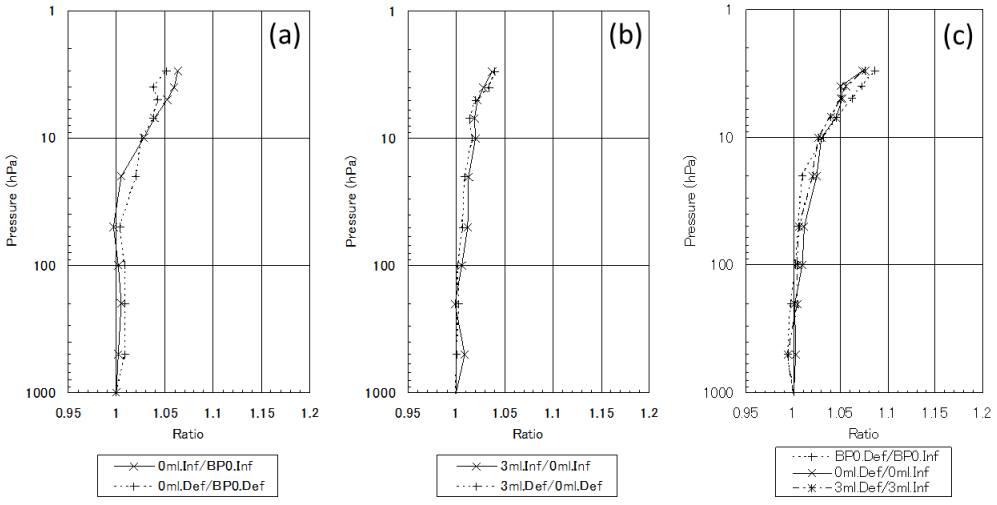

Figure 8: (a) Ratio of pump efficiency when connected directly to the flowmeter from the pump exhaust port and through an empty reaction cell. (b) Ratio of pump efficiency between the case of an empty reaction cell and the case of adding 3 ml of reaction solution, which is the standard amount of ECC type reaction solution. (c) Ratio of pump efficiency during inflation and deflation under the same load conditions. Inf: Inflation, Def: Deflation, BP0: Back pressure 0hPa, 0ml: Reaction solution 0 ml, 3ml: Reaction solution 3 ml.

From the discussion in the previous paragraph, we conclude that a filled reaction cathode cell generates a back pressure, hereby affecting the pump efficiency, as in real atmospheric conditions. Figure 9 reveals investigation results revealing the correlation of the back pressure versus solution volume in the cell at the ground level pressure. According to this, the back pressure is about 3 hPa for the standard ECC-type reaction solution volume of 3 ml. To reproduce this load, the length and diameter of the piping were adjusted, and a load of 3 hPa was successfully applied to the exhaust side without adding any reaction solution to the cell.

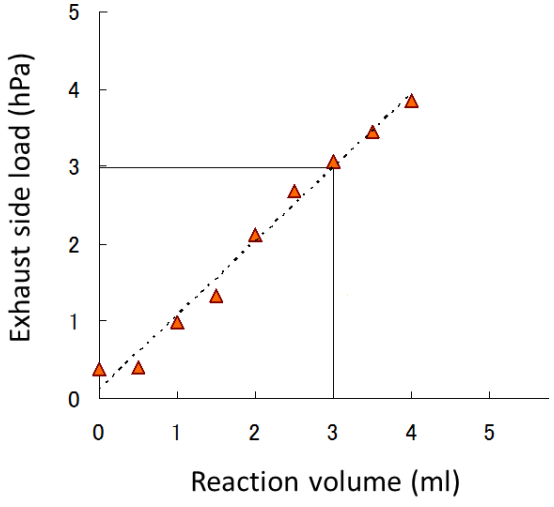

Figure 9: Exhaust side load when using a reaction cell. 3 ml of standard reaction solution is equivalent to a load of about 3 hPa.

https://doi.org/10.5194/egusphere-2022-565
Preprint. Discussion started: 19 August 2022

4 Method of calculating the pump correction factor

As mentioned in the previous section, there are some factors that can cause various observation errors in pump efficiency measurements. In this section, we explain the correction method to remove those errors.

4.1 Correction for the effect of heat generation in the pump

The series of pump efficiency measurements starts from the ground level pressure and continues with lower pressures. As the pump motor gradually heats up due to friction, the air exhaled (sucked out) from the pump becomes warmer in the later stages of the measurement. The volume change caused by the heating of the inflowing air is a source of error in the measurement results, and should therefore be corrected for. Since the heat capacity of the air discharged from the pump is sufficiently small, we assume that the air is warmed to the same temperature as the pump temperature while passing through the pump, and the initial pump correction factor $pcf_0(p, \Delta p)$ is adjusted as follows,

$$pcf_1(p, \Delta p) = pcf_0(p, \Delta p) \frac{T_{pump}(p_0, \Delta p=0.8)}{T_{pump}(p, \Delta p=0.8)}, \quad (4)$$

where $T_{pump}(p, \Delta p)$ is the pump temperature (K) at differential pressure Δp at air pressure p (p_0 is the ground level pressure). Here, these temperatures are the values when the differential pressure is 0.8 hPa (at the most inflated state).

4.2 Correction for the effect of differential pressure

The measurement time is defined as the time required for the pump to exhaust the air and inflate the airbag from from zero volume to V_{airbag} or to deflate it from V_{airbag} to zero, under atmospheric pressure p. However, the air actually pumped into the airbag is further inflated (deflated) by the amount of differential pressure $\pm\Delta p$ in addition to the ambient air pressure p. We should consider the effect of this on the measurement time by converting the air pressure change inside the airbag into a volume change. Assuming no change in temperature, using the Boyle-Charles law, the internal volume of the airbag, V_{airbag}, changes by the ratio of the airbag differential pressure Δp, to the ambient air pressure p, so the measurement time t_m for the net measurement time $t(p)$, at the air pressure p is expressed as

$$t_m = t(p) \cdot (1 + \Delta p/p). \quad (5)$$

From this equation, we can see that the lower the ambient pressure p is, the larger the effect on the measurement time. To confirm the effect of this correction (hereafter referred to as the pressure correction) using t_m as the measurement time, we varied the differential pressure threshold from ±0.1 to ±0.8 hPa in turn, obtained the pump efficiency with this correction for each pressure, and compared it with that without the correction. Figure 10 shows the comparison results at ambient pressure of 3 hPa. It can be seen that the pressure correction generally does a good job, but, even after applying this correction, the correlation between the pump correction factor and the differential pressure threshold remains high. We consider the effect of the differential pressure acting as another load factor on the pump. In other words, if the differential pressure acts as the exhaust

https://doi.org/10.5194/egusphere-2022-565
Preprint. Discussion started: 19 August 2022

(intake) side load when the airbag is inflated (deflated), it is consistent with the results of the previous pressure correction. However, deriving correction for this effect is not straightforward, because these loads change during measurement and different pumps respond differently to those loads. To avoid such effects, we should make measurements at even lower differential pressure thresholds, but there is a limitation to the differential pressure thresholds that can be set, very small differential pressures are outside the detection limit of the micro differential pressure gauge and the measurement of time intervals is prone to errors. On the other hand, since the pump correction factor without differential pressure correction shows a very high correlation with the differential pressure threshold, we can fully use the y-intercept of the regression line as an estimate of the pump correction factor for a zero differential pressure threshold. Therefore, in the actual measurement, we estimate the pump correction factor corrected for the effect of the differential pressure by the regression line obtained from the measurement time taken at each of the multiple differential pressure thresholds. The pump correction factor $pcf_2(p)$ at zero differential pressure obtained by the method described above is expressed as

$$pcf_2(p) = pcf_1(p, \Delta p = 0). \quad (6)$$

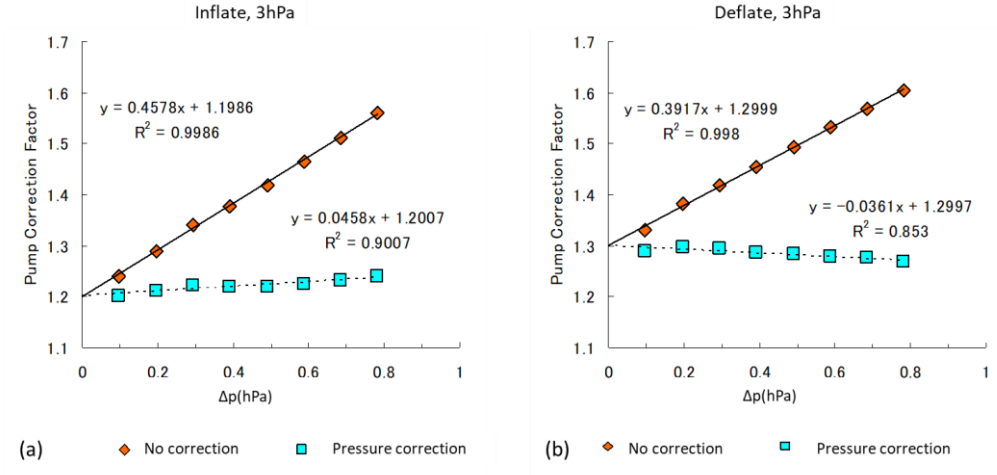

Figure 10: Pump correction factor for different differential pressure thresholds. The pump correction factors (inverse of pump efficiency) calculated for each differential pressure threshold are plotted without correction and with pressure correction. The values in (a) and (b) are based on the measurement time during expansion and contraction, respectively, at 3 hPa ambient air pressure. These values were measured by connecting the pump's inlet and exhaust ports directly to a flowmeter.

4.3 Correction for the changes in airbag capacity due to temperature

The airbag used for differential pressure measurement is made of polyethylene. Since polyethylene has the property of expanding and contracting depending on the temperature, we need to consider the change in the volume of the airbag during measurement. The temperature inside the airbag gradually rises during measurement because the piping leading to the airbag is heated by the heat of the solenoid valve and circuit board inside the flowmeter housing, and the air pumped into the airbag is heated by the frictional heat of the pump. The temperature eventually rises by about 5 to 10°C in a measurement sequence.

https://doi.org/10.5194/egusphere-2022-565
Preprint. Discussion started: 19 August 2022

Since this variation in airbag volume is also a measurement error source, the pump efficiency is corrected using temperature data obtained from thermistors placed near the airbag.

After measuring the pump efficiency while changing the temperature inside the airbag in a thermostatic bath, we found that about half of the airbag temperature change rate affected the pump correction factor. Based on the results of this experiment, the pump correction factor after correction for the temperature-dependent change in airbag capacity is expressed as follows,

$$pcf_3(p) = pcf_2(p)\left(1 - 0.5\frac{T_{airbag}(p_0,\Delta p=0.8) - T_{airbag}(p,\Delta p=0.8)}{T_{airbag}(p_0,\Delta p=0.8)}\right), \quad (7)$$

where $T_{airbag}(p, \Delta p)$ is the temperature of the airbag (K) at differential pressure Δp at air pressure p (p_0 is the ground level pressure).

4.4 Application of pump efficiency measurement results to ozone partial pressure calculation

The pump efficiency $k(p)$ at atmospheric pressure p is given by the following equation (Kobayashi, Toyama; 1966),

$$k(p) = 1 - K \cdot \left(\frac{1}{p} - \frac{1}{p_0}\right),$$

where p_0 is the ground level pressure (hPa) and K is constant. According to Steinbrecht et al. (1998), when adiabatic change occurs in the pump, a power term (specific heat ratio $\gamma \approx 1.4$) is added to the second term on the right side as follows,

$$k(p) = 1 - K \cdot \left(\frac{1}{p} - \frac{1}{p_0}\right)^{\frac{1}{\gamma}}.$$

From above, the following approximate expression is given as

$$pcf(p) = \frac{1}{1 - c_0\left(\frac{1}{p} - \frac{1}{p_0}\right)^{c_1}}. \quad (8)$$

The application of the pump efficiency measurement results to the ozonesonde observations is based on $pcf_3(p)$ with the corrections described in section 4.3. $pcf_3(p)$ is calculated from the average of 6 measurements in total, 3 times each during inflation and deflation at each specified atmospheric pressure of 200 hPa or less. Using this equation, c_0 and c_1 of the approximate expression (8) are obtained by fitting. The pump correction factor $pcf(p)$ at pressure p is then calculated from the approximate equation (8) using the obtained constants c_0 and c_1. Note that we do not use ground pressure data because $pcf_3(p)$ should be 1.

5 Pump efficiency data operationally obtained by the JMA's automated pump efficiency measuring system

Since 2009, JMA has been conducting a complete inspection of EN-SCI ECC ozone sensor's pump efficiency with the automated pump efficiency measurement system, and has been using the pump correction factor calculated from the

https://doi.org/10.5194/egusphere-2022-565
Preprint. Discussion started: 19 August 2022

measurement results to correct the ozonesonde observations at the Sapporo, Tateno, and Naha stations. This section presents the results of measurements made over this last 13 years.

5.1 Comparison of pump correction factor between JMA and other organizations

Figure 11 shows the results of pump correction factor measurements at Sapporo, Tateno, and Naha from 2009to 2022. Sensors with similar serial numbers had been used at each station. The pump correction factors were generally consistent among the stations, although the difference was slightly larger at 3 hPa, where the measurement accuracy is lower.

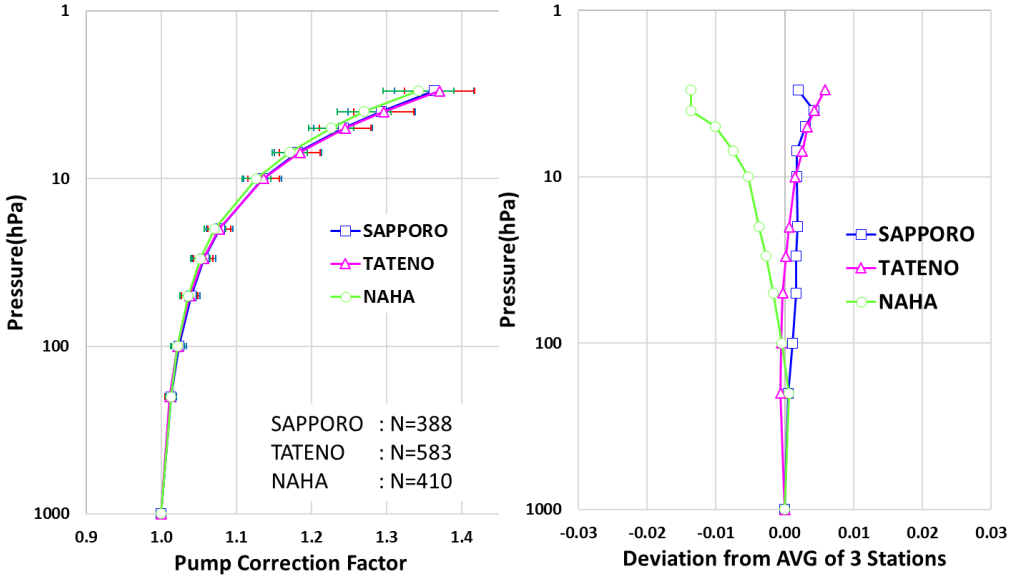

Figure 11: Pump efficiency measurement results in Sapporo, Naha from 2009 to 2018, and Tateno from 2009 to 2022. The error bars in the left figure represent the one sigma standard deviation. The results measured at 3 sites are almost synchronized.

Figure 12 shows the results comparing the average pump correction factors of the same pump type (EN-SCI ECC) obtained by other organizations with the representative measured data of JMA. The pump motor specifications were changed from the ozone sensor (serial number 24000 or later) delivered to JMA in 2013. As a result, air pressure dependence was seen in the motor speed, and the stability of the speed was not good. We thought that the effect was affecting the pump efficiency. Therefore, the measurement results of sensors with serial number 24000 and above are used to calculate the representative data of JMA. Stauffer et al. (2020) also presents the discovery of an apparent instrument artifact that has caused total ozone measurements from about a third of global stations to drop starting in 2014–2016, limiting their suitability for calculating ozone trends.

The measurements at the University of Wyoming have been performed without any exhaust-side loading by the reaction solution, and NOAA/CMDL has made measurements with exhaust-side loading by the reaction solution (Johnson et al., 2002).

https://doi.org/10.5194/egusphere-2022-565
Preprint. Discussion started: 19 August 2022

We did that with 3 ml reaction solution. According to these comparisons, the pump correction factors during expansion are close to the values obtained by other organizations, and the tendency with the ambient air pressure is also similar. These suggest that the newly developed measurement system is working well.

These measured pump flow efficiencies significantly differ from those published in Komhyr et al. (1995). This is because, as noted by Smit et al. (2021), pump efficiencies in Komhyr et al. (1995) in fact represent an overall correction that includes both the pump flow efficiency and an estimate of the stoichiometry increase over the flight.

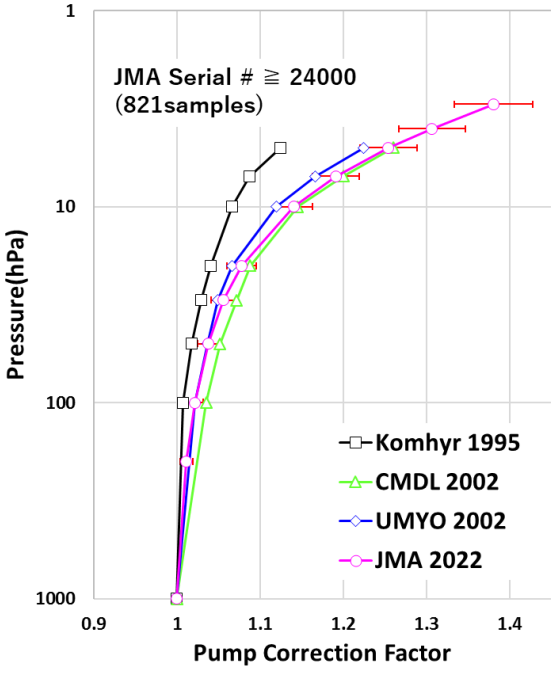

Press.	Pump Correction Factor [JMA 2022]
3	1.381 ± 0.047
4	1.307 ± 0.040
5	1.254 ± 0.034
7	1.191 ± 0.028
10	1.140 ± 0.023
20	1.078 ± 0.017
30	1.056 ± 0.015
50	1.038 ± 0.013
100	1.021 ± 0.010
200	1.011 ± 0.008

Figure 12: Comparison of pump correction factors by our airbag method with other experiments. Curves of pump correction factors as a function of pressure are represented for the standard Komhyr et al. (1995) is marked by a black line with squares and JMA pump correction factor is marked by a red line with circles. The error bars represent the one sigma standard deviation. Also, a curve using the NOAA/CMDL average oil bubble flowmeter is marked by a green line with triangles, and that using the Wyoming bag method is marked by a blue line with rhombuses (Johnson et al., 2002).

5.2 Long-term stability of the system

We have investigated the long-term stability of the measurement system by evaluating results of multiple measurements on a sample of 4 pumps investigated at the Aerological Observatory in Tateno from 2010 to 2021. In addition to the correction explained in section 4, we have corrected the pump correction factor according to the pump motor speed as shown in the following formula in order to eliminate biases between the pump correction factors between the different uses of the same pump,

$$pcf_{corr}(p) = pcf(p)\frac{MS(p_0)}{MS(p)}, \quad (9)$$

https://doi.org/10.5194/egusphere-2022-565
Preprint. Discussion started: 19 August 2022

where $pcf_{corr}(p)$ is the pump correction factor after motor speed correction at air pressure p, $pcf(p)$ is the pump correction factor before motor speed correction at atmospheric pressure p and $MS(p)$ is the motor speed at atmospheric pressure p (p_0 is the ground level pressure). Figure 13 show these multiple pump flow correction factors for a sample of 4 pumps. As can be seen, there is no increasing nor decreasing trend in the pump correction factors for neither of the pumps, although individual differences exist. This illustrates the long-term stability of the measurement system and the absence of any aging degradation effect.

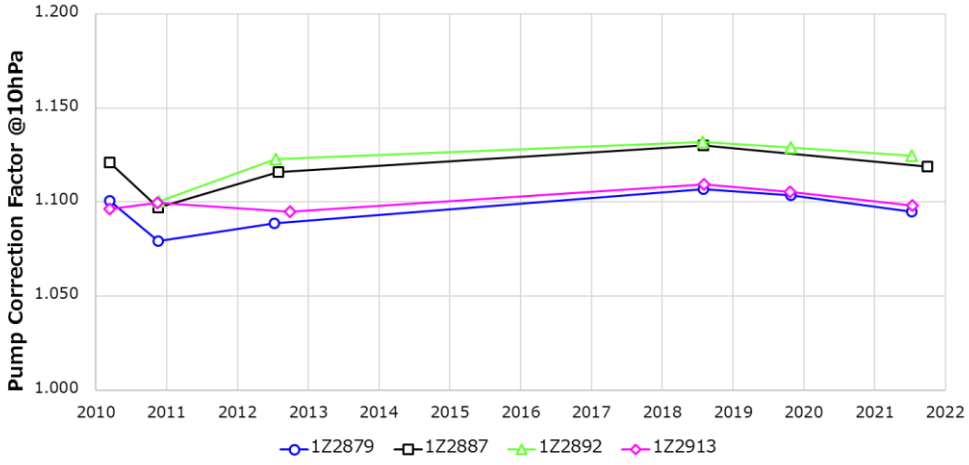

Figure 13: Pump correction factors at 10 hPa measured by the same sensor during the period 2010-2021. Four sensors were used for the measurements.

5.3 Decadal monitoring on individual pump efficiency

Figure 14 shows the time series of individual pump correction factors at 50, 20, and 10 hPa measured at Sapporo, Tateno, and Naha stations from 2009 to 2022 (Sapporo and Naha terminated their ozonesonde observations in February 2018). At all stations, the pump correction factor changes with time, showing a slightly increasing trend although with different slopes. The slope is larger with lower ambient pressure to around 2018-2019 (Sapporo:+1%/9 years, Tateno:+1%/decade, Naha:+1% or less /9 years at 50 hPa, Sapporo:+2%/9 years, Tateno:+2%/decade, Naha:+2%/9 years at 20 hPa, and Sapporo:+4%/9 years, Tateno:+4%/decade, Naha:+2%/decade at 10 hPa). The serial numbers of the ozone sensor used at each station were fairly balanced. As the pump efficiency measurement system turned out to be very stable (section 5.2), these trend of the pump correction factors should be ascribed to the ozonesonde pumps themselves.

https://doi.org/10.5194/egusphere-2022-565
Preprint. Discussion started: 19 August 2022

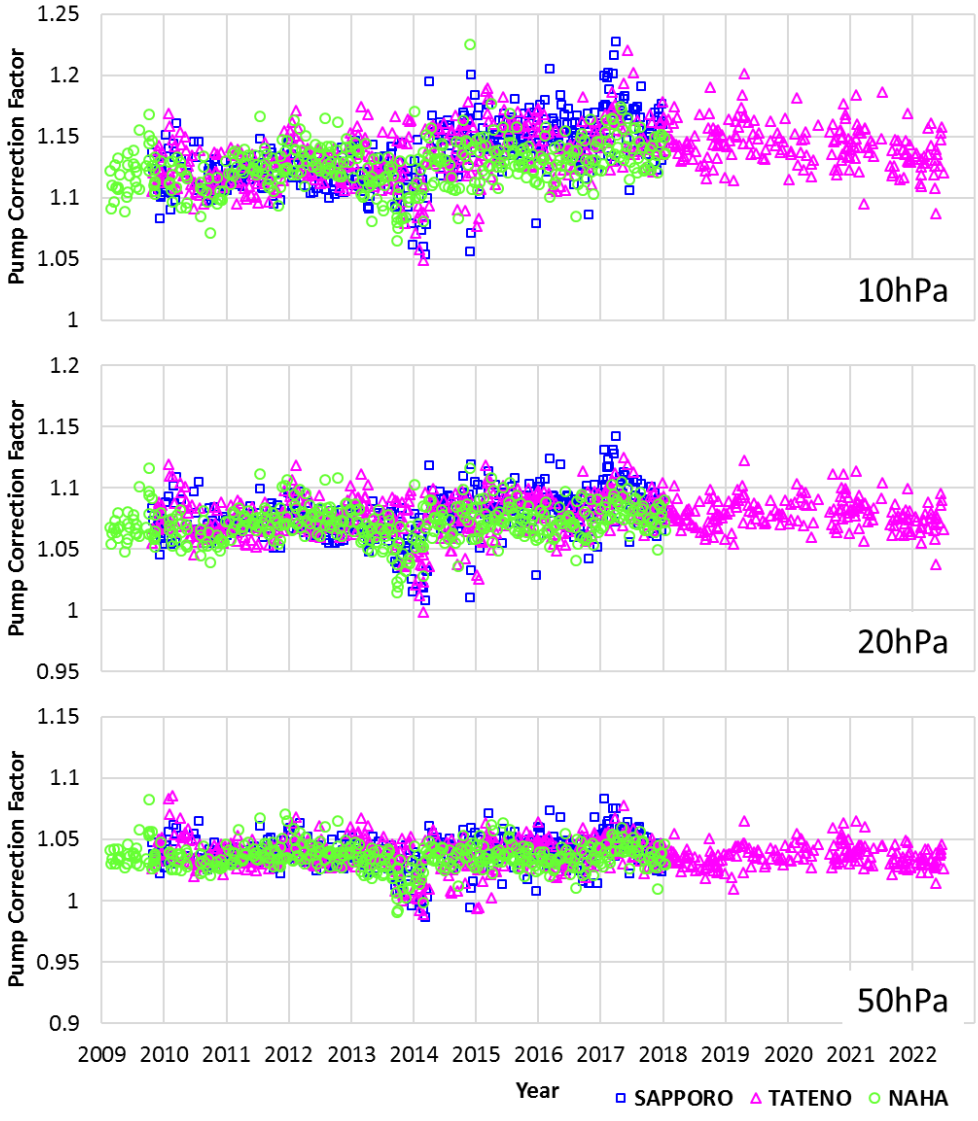

Figure 14: Pump correction factors measured for the period 2009-2022. From top to bottom, 10 hPa, 20 hPa, and 50 hPa. In 11 years, the pump correction coefficient has changed by + 1% at 50hPa, + 2% at 20hPa, and + 4% at 10hPa.

To further confirm whether this trend is caused by the pump or not, we present the pump correction factors for the different stations as a function of the ozonesonde serial number in Fig. 15a. In Fig. 15b, the pump correction factors at 10 hPa are averaged for bins of 1000 of the serial numbers. From those figures, we confirm that the variability of the pump correction factors within a production lot is rather modest (1.8%) and that differences between different production lots are mostly statistically insignificant.

https://doi.org/10.5194/egusphere-2022-565
Preprint. Discussion started: 19 August 2022

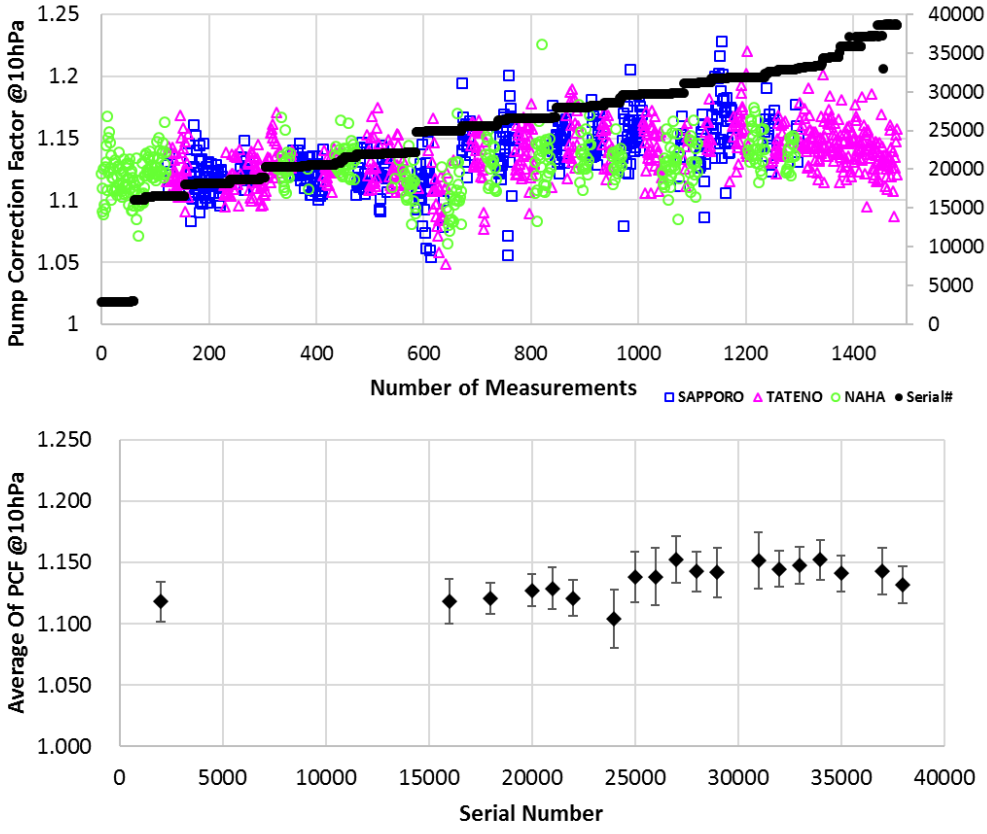

Figure 15: (Upper) Pump correction factor and ozone sensor serial number at 10hPa measured during 2009-2019. (Lower) Pump correction factor at 10 hPa averaged for each bin of 1000 of ozonesonde serial numbers measured during the period 2009-2022. The error bars in the figure below represent the one standard deviation.

Figure 16 shows a comparison of the measured values of the pump flow rate, motor speed, and pump stroke obtained by dividing the flow rate value by the motor speed value at the ground level pressure and 10 hPa. Although there is no significant change in the measured flow rate, the pump motor speed increased by about 5 to 10% and the pump stroke decreased by 5 to 10% after the sensor serial number 24000. We infer that the pump stroke got shorter might increase the relative volumetric ratio of the pump dead space to the piston volume due to the change of the motor specifications after the serial number 24000 as described in section 5.1. This might be the origin of a worse pump efficiency. Furthermore, focusing on the deviations between the ground level pressure and 10 hPa measurements, there is little change in the motor speed differences, but with a trend in the pump flow rate and pump stroke differences. From this, we consider that the difference in pump flow rate changes between the ground and the lower pressure, that is, the difference in measurement time changes, resulting in an increase in the pump correction factor. In any case, the motor characteristics fluctuate discontinuously after the serial number 24000, and the flow rate and other characteristics of the ozone sensor change with each group of sensor serial numbers. Therefore, we consider that the increasing trend of the pump correction factor is largely due to the sensor side.

https://doi.org/10.5194/egusphere-2022-565
Preprint. Discussion started: 19 August 2022

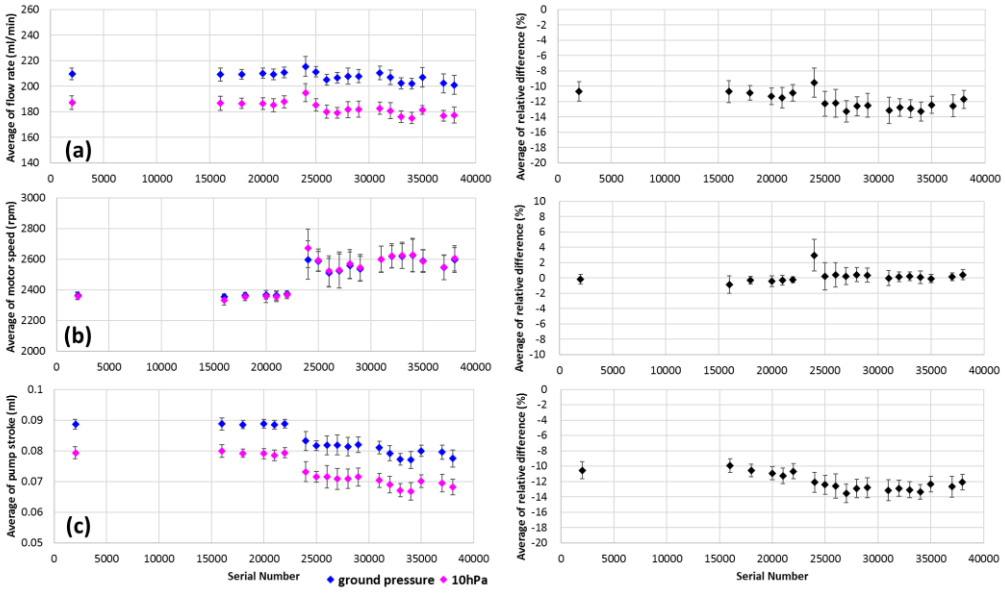

Figure 16: Variation over time of pump flow rate (a), pump motor speed (b), and pump stroke (c) at ground pressure and 10 hPa averaged for each serial number of ozone sensors measured during the period 2009-2022 (left column: measured average values, right column: relative difference to values at ground pressure).

5.4 Influence on the estimation of ozone concentration

We will consider the effect of the variability caused by the changes in the characteristics of the pump flow rate introduced so far on the observed data of total ozone. Fig. 17 shows the relative differences of total ozone integrated values to the average that value. The total ozone integrated values are determined using the ozone partial pressure values obtained by multiplying the pump correction factor measured during the period from 2009 to 2022 for each pressure levels (the ground level pressure, 500, 200, 100, 50, 30, 20, 10, 7, 5, 4 hPa) by the average ozone partial pressure from 1994 to 2008 corresponding to that pressure level. We confirmed that the variation in total ozone was reached about 4% in the largest case. The standard deviation in the relative differences of total ozone integrated values by lot was about 1%, and that between production lots was about 0.6%.

https://doi.org/10.5194/egusphere-2022-565
Preprint. Discussion started: 19 August 2022

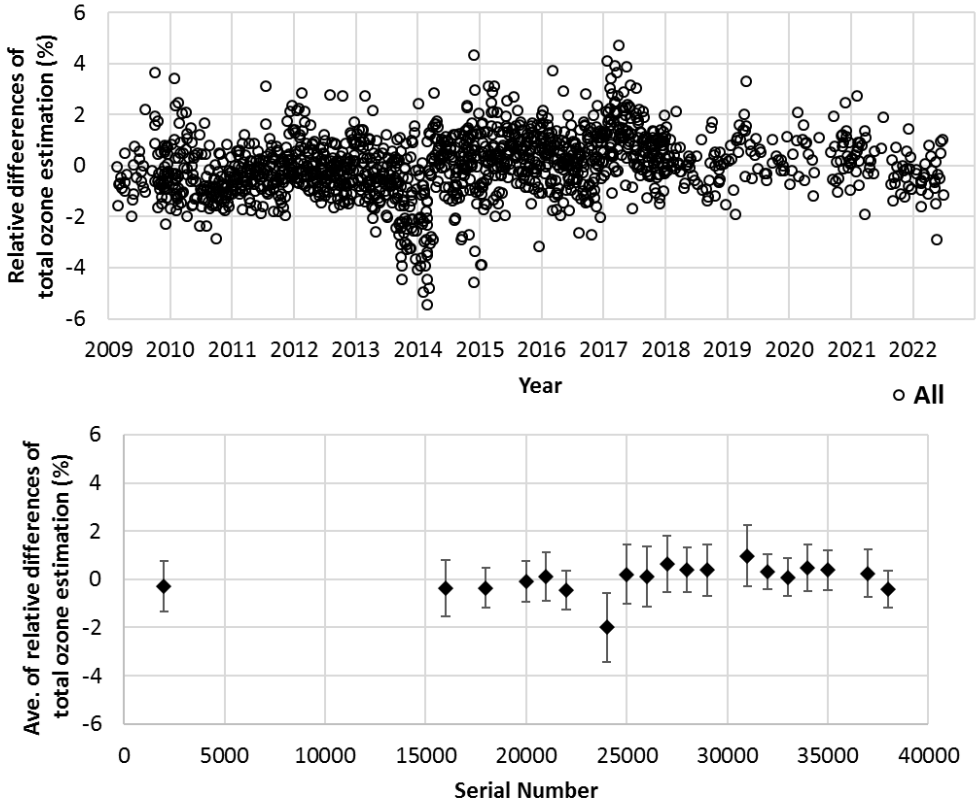

Figure 17: (Upper) Relative differences of total ozone integrated values obtained from the pump correction factor measured during the period 2009-2022 and the average ozone profile (1994-2008 cumulative average). (Lower) Average of the total ozone integrated values averaged for each serial number.

6 Conclusion

JMA has succeeded in developing a unique system for measuring pump efficiency, and has enabled to measure the pump efficiency of individual ECC ozonesondes fully automatically. Based on the time series of the individual pump correction factors of the EN-SCI ozonesonde that have been calculated by JMA using this system, we found that the factors changed over time with an increasing tendency, and also that they varied depending on the production lot. We can attribute this to differences in the characteristics of mechanical pumps and pump motors for each production lot. In this situation, if a table of correction values for the pump flow rate correction factor is used without individual pump efficiency measurements, the total ozone value will be affected by up to about ±4%.

Systematic biases introduced in ozonesonde observations due to a change in the pump performance can lead to erroneous stratospheric vertical ozone trend values. In order to avoid the influence of the lot-dependent pump correction factor of EN-SCI's ozonesondes on the stratospheric ozone trend and to detect the actual atmospheric change with high accuracy, we

https://doi.org/10.5194/egusphere-2022-565
Preprint. Discussion started: 19 August 2022

recommend to investigate the pump efficiency of each lot to understand the trend of the pump correction factor and to adapt it to the calculation of ozone concentration.

Code and Data availability

Code and data from this study are available upon request to the author.

Competing interests

The contact author has declared that neither they nor their co-authors have any competing interests.

Author contribution

TN led conceptualization and development of the automated pump efficiency measuring system. TM and TN led the analyses presented here and prepared the paper.

References

Johnson, B. J., Oltmans, S. J., Voemel, H., Smit, H. G. J., Deshler, T., and Kroeger, C.: ECC Ozonesonde pump efficiency measurements and tests on the sensitivity to ozone of buffered and unbuffered ECC sensor cathode solutions, J. Geophys. Res., 107, D19 doi: 10.1029/2001JD000557, 2002.

Kobayashi, J., and Toyama, Y.: On various methods of measuring the vertical distribution of atmospheric ozone（III）–Carbon iodide type chemical ozonesonde–, Pap. Meteor. Geophys., 17, 113–126, 1966.

Komhyr, W. D.: Electrochemical concentration cells for gas analysis, Ann. Geophys., 25, 203-210, 1969.

Komhyr, W. D.: Development of an ECC-Ozonesonde, NOAA Techn. Rep., ERL 200-APCL 18ARL-149, 1971.

Komhyr, W. D.: Operations handbook - Ozone measurements to 40 km altitude with model 4A-ECC-ozone sondes, NOAA Techn. Memorandum ERL-ARL-149, 1986.

Komhyr, W. D., Barnes, R. A., Brothers, G. B., Lathrop, J. A., and Opperman, D. P.: Electrochemical concentration cell ozonesonde performance evaluation during STOIC 1989, J. Geophys. Res., 100, 9231-9244, 1995.

Smit, H. G. J., and the Panel for ASOPOS: Quality Assurance and Quality Control for Ozonesonde Measurements in GAW, WMO GAW Rep. 201, 94pp, https://library.wmo.int/doc_num.php?explnum_id=7167, 2014.

Smit, H. G. J., Thompson, A. M., and the ASOPOS 2.0 Panel: Ozonesonde measurement principles and best operational practices - ASOPOS 2.0 (Assessment of Standard Operating Procedures for Ozonesondes), World Meteorological Organization GAW Rep. 268, 172pp, https://library.wmo.int/doc_num.php?explnum_id=10884, 2021.

https://doi.org/10.5194/egusphere-2022-565
Preprint. Discussion started: 19 August 2022

Stauffer, R. M., Thompson, A. M., Kollonige, D. E., Witte, J. C., Tarasick, D. W., Davies, J., Vömel, H., Morris, G. A., van Malderen, R., Johnson, B. J., Querel, R. R., Selkrik, H. B., Stübi, R., and Smit, H. G. J.: A Post-2013 Dropoff in Total Ozone at a Third of Global Ozonesonde Stations: Electrochemical Concentration Cell Instrument Artifacts?, Geophysical Research Letters, 47, e2019GL086791. doi:10.1029/2019GL086791, 2020.

Steinbrecht, W., Schwarz, R., and Claude, H.: New pump correction for the Brewer–Mast ozone sonde: Determination from experiment and instrument intercomparisons, J. Atmos. Ocean. Tech., 15, 144-156, https://doi.org/10.1175/1520-0426(1998)015%3C0144:NPCFTB%3E2.0.CO;2, 1998.

World Ozone and Ultraviolet Radiation Data Centre: Dataset Information: OzoneSonde, http://dx.doi.org/10.14287/10000008.